OL Organic Letters

pubs.acs.org/OrgLett

Letter

Photochemical Construction of Trifluoromethyl Bicyclo[1.1.1]pentyl-heterocycles

Marta Gil-Ordóñez, Albert Gallego-Gamo,† Yingmin Ji,† Tapas Maity, Remy Lalisse, Elies Molins, Roser Pleixats, Carolina Gimbert-Suriñach,* Adelina Vallribera,* Osvaldo Gutierrez,* and Albert Granados*

Cite This: *Org. Lett.* 2026, 28, 248−253

Read Online

ACCESS | Metrics & More | Article Recommendations | Supporting Information

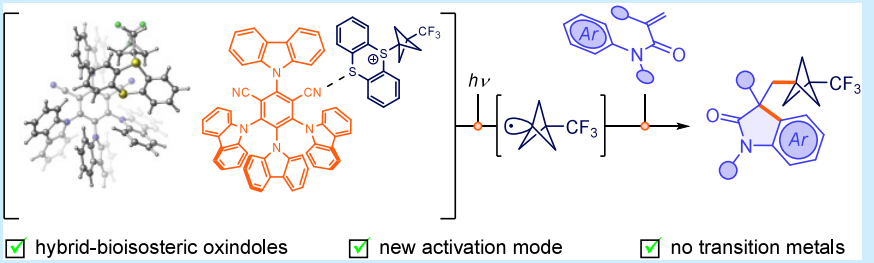

ABSTRACT: We describe a transition-metal-free photocatalytic synthesis of CF_3−BCP−oxindoles via radical cascade annulation. This mild and sustainable protocol employs a bench-stable thianthrenium CF_3−BCP reagent and activated anilides under visible-light irradiation to efficiently assemble complex scaffolds bearing dual (CF_3 and BCP) bioisosteric features. Mechanistic studies reveal that CF_3−BCP radical generation proceeds through a previously unreported electron donor−acceptor (EDA) complex between 4CzIPN and the thianthrenium salt, initiating a radical chain process. This method provides a practical photochemical platform for the late-stage incorporation of CF_3−BCP motifs into oxindole frameworks and expands the accessible bioisosteric chemical space for drug discovery.

Scheme 1. (A) Comparison of *para*-Substituted Arenes and 1,3-Disubstituted BCPs, (B) Photochemical Methods Using Bicyclo[1.1.1]pentyl-thianthrenium Reagents, and (C) Our Work[a]

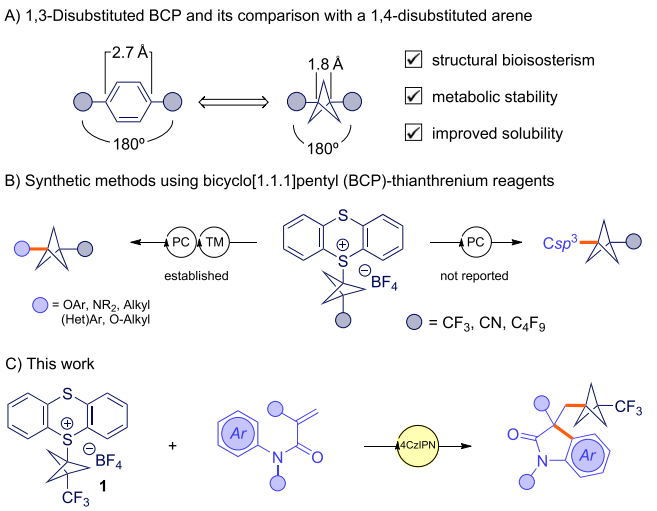

[a]PC, photocatalyst; TM, transition metal.

Within medicinal chemistry settings, the 100% C(sp^3)-hybridized and rigid bicyclo[1.1.1]pentane (BCP) scaffold has gained recognition as a competent bioisostere for monosubstituted phenyl and 1,4-disubstituted phenyl motifs in numerous cases, attracting increasing attention.[1] Particularly, 1,3-disubstituted BCPs can mimic the spatial orientation of *para*-substituted phenyl rings, albeit with a slightly shortened distance between the two substituents (Scheme 1A).[2] This arises from the high fraction of sp^3 carbons, which confers enhanced metabolic stability due to the absence of π bonds that are prone to oxidative metabolism. Additionally, the three-dimensional structure of BCPs reduces the likelihood of $\pi-\pi$ stacking interactions observed with phenyl rings, resulting in improved solubility in physiochemical environments.[3] Pioneering works by Pellicciari[4] and Pfizer[5] highlighted the unprecedented bioisosteric properties of BCP units. Since then, interest in incorporating BCP scaffolds into

Received: November 6, 2025
Revised: December 12, 2025
Accepted: December 16, 2025
Published: December 23, 2025

Table 1. Substrate Scope Study[a]

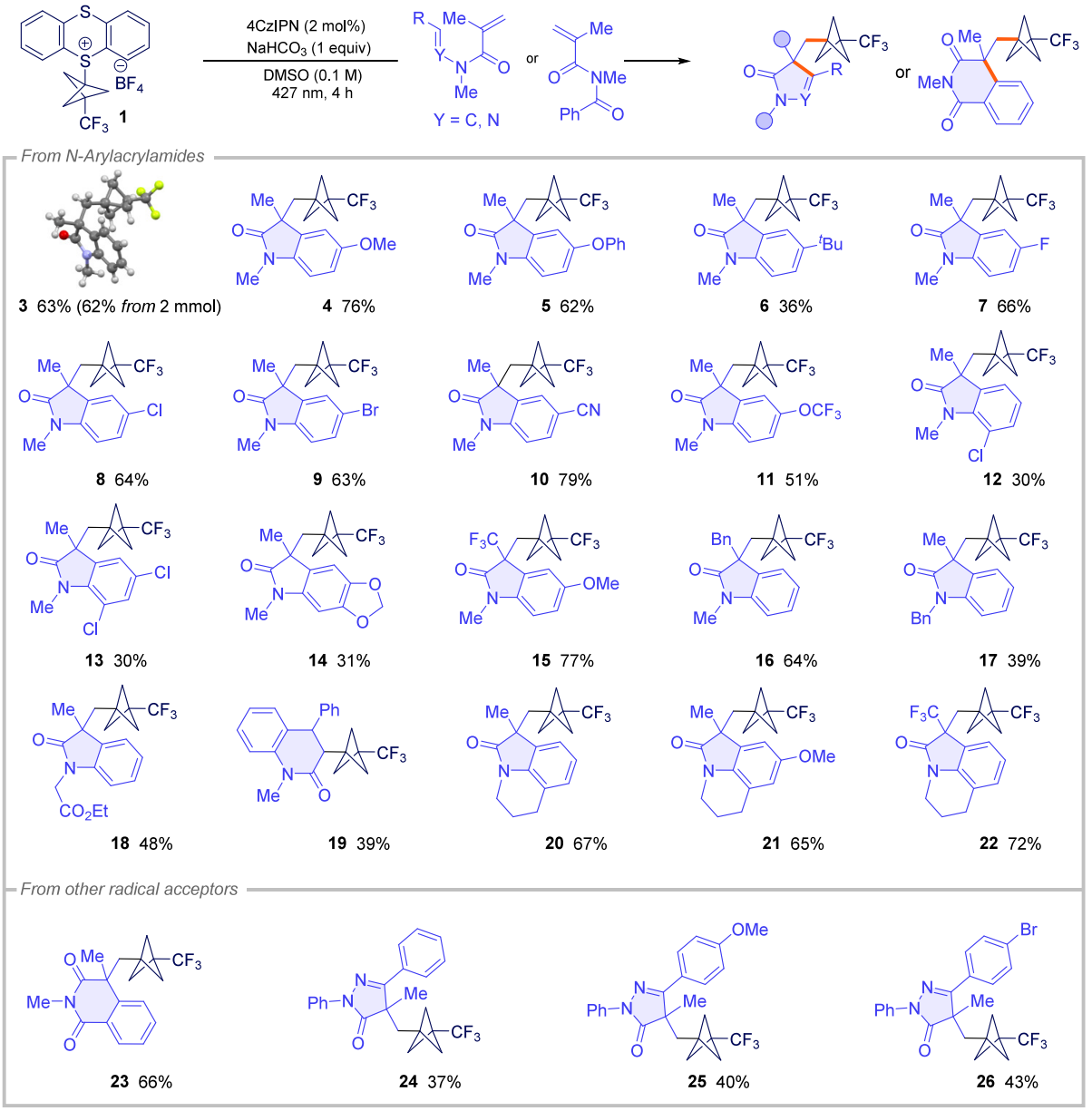

[a]Reaction conditions: **1** (0.25 mmol, 1 equiv), **2a** (2 equiv), $NaHCO_3$ (1 equiv), and 4CzIPN (2 mol %) in 2.5 mL of DMSO (0.1 M) under violet Kessil lamp irradiation (λ_{max} = 427 nm) at rt for 4 h.

small-molecule drugs has skyrocketed, alongside significant advances in synthetic methods for accessing a variety of BCP-containing molecules,[6] including photoinduced methods.[7] The trifluoromethyl (CF_3) group is likewise a privileged bioisostere widely used to modulate lipophilicity, metabolic stability, and binding affinity and is routinely incorporated during fluorine scan stages of drug discovery.[8,9] Combining BCP and CF_3 units offers the potential to generate new chemotypes with enhanced pharmacological profiles. However, general methods for assembling such dual bioisosteres remain limited.[10]

Herein, we report a photocatalytic strategy for accessing CF_3−BCP-containing oxindoles (Scheme 1C). Oxindoles are prevalent in pharmaceuticals and natural products,[11] yet integration of the BCP motif into this framework has not been explored.[12] The transformation proceeds through a photochemical radical cascade between activated anilides and bench-stable thianthrenium CF_3−BCP reagent **1**. Although **1** has been applied in metallaphotoredox cross-couplings to construct C−O, C−N, and C−C bonds (Scheme 1B),[13] its addition to π systems has not been demonstrated. This method therefore expands both the synthetic space of oxindole scaffolds and the reactivity profile of the CF_3−BCP radical under metal-free conditions.

We began our study using thianthrenium salt **1** and *N*-arylacrylamide **2a** as model substrates (Table S1). Preliminary experiments indicated that a photocatalyst was required to enable productive reactivity. Systematic variation of the photocatalyst, base, and reaction parameters (see Table S1) identified 4CzIPN and $NaHCO_3$ as optimal, delivering oxindole **3** in up to 76% yield after 4 h of irradiation, and control studies confirmed that light is essential for the transformation. The molecular structure of oxindole **3** was

https://doi.org/10.1021/acs.orglett.5c04624
Org. Lett. 2026, 28, 248−253

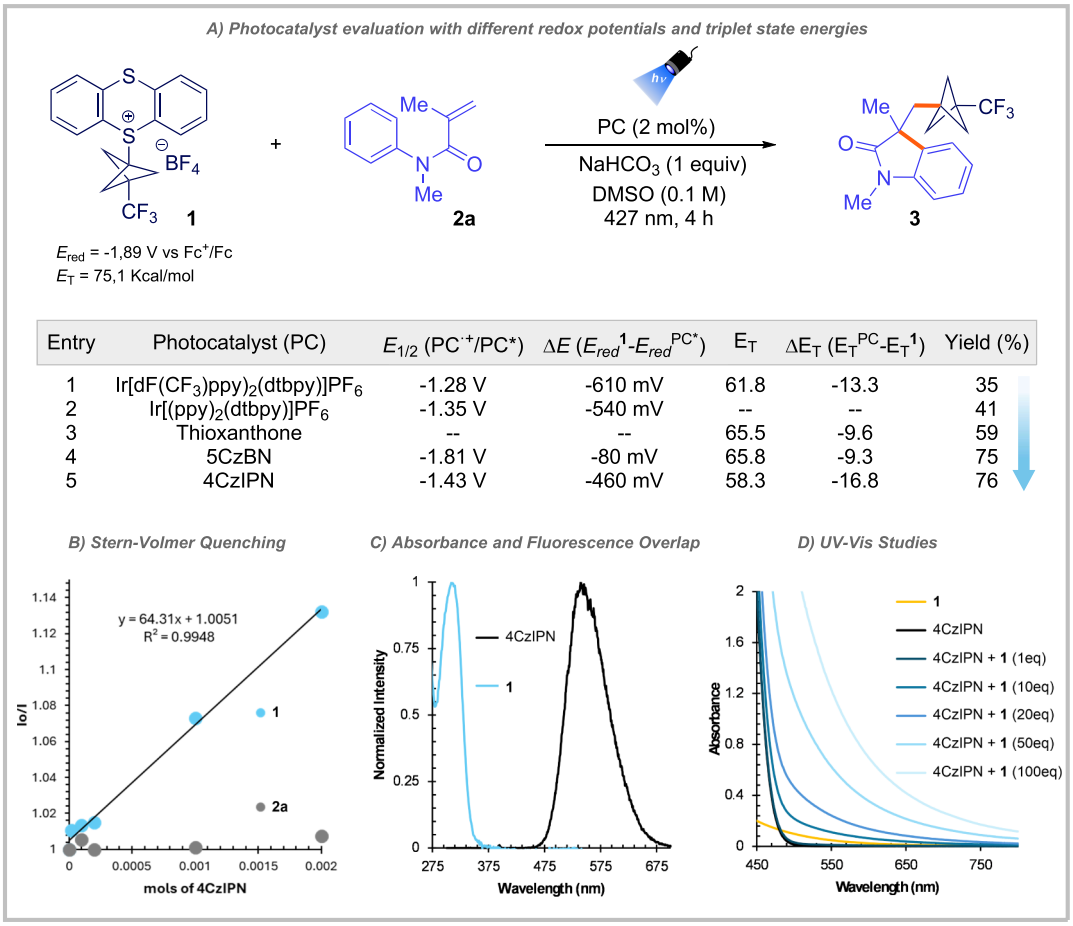

Figure 1. (A) Redox potentials[17] (vs Fc^+/Fc), triplet-state energies[18] (E_T in kcal/mol), and reaction yields for the series of photocatalysts (PCs), (B) fluorescence quenching experiment using 4CzIPN (2 mM in DMSO), (C) normalized UV−vis of **1** in DMSO (blue line) and fluorescence spectra of 4CzIPN in DMSO (black line), and (D) UV−vis studies performed using 4CzIPN (2 mM in DMSO).

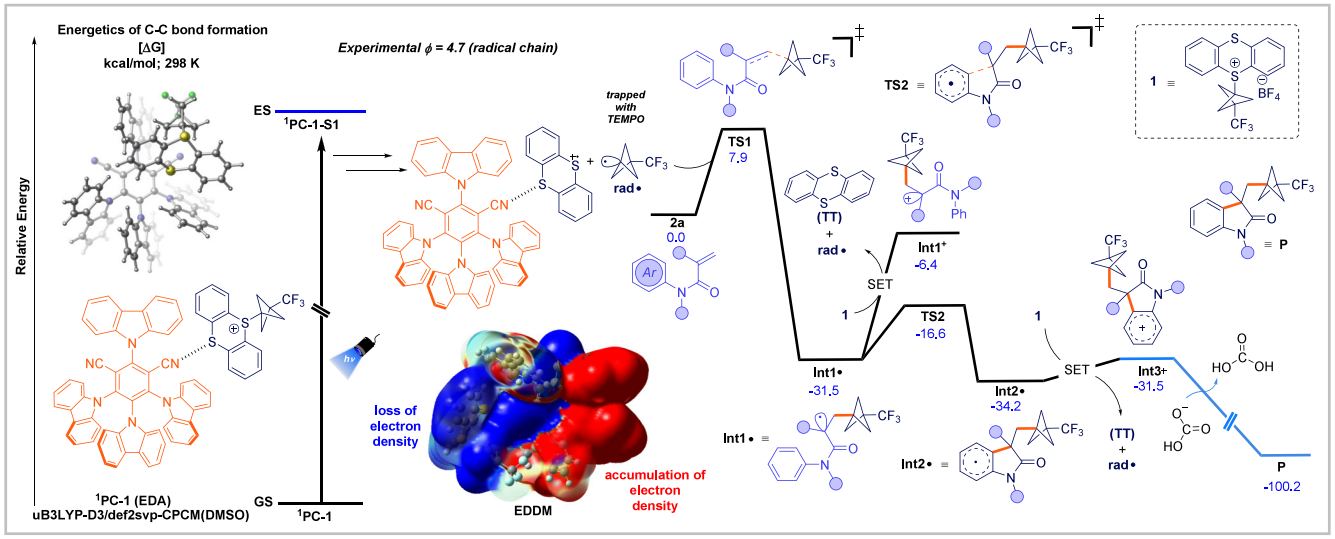

Figure 2. Potential energy surface of the radical chain pathway after radical activation from PC−**1** calculated at the UB3LYP/def2svp-CPCM(DMSO) level of theory. Energies are given in blue in kcal/mol.

unambiguously established by single-crystal X-ray diffraction, definitively confirming the presence of the CF_3−BCP motif tethered in the oxindole core. The folded conformation of the molecule is favored by an intramolecular H···π interaction among BCP and the five-membered ring (see section 5 of the Supporting Information). To the best of our knowledge, this represents the first example of reagent **1** being employed exclusively with a photocatalyst, without the participation of other metals, such as nickel or copper, in an efficient fashion.

https://doi.org/10.1021/acs.orglett.5c04624
Org. Lett. 2026, 28, 248−253

With the optimized conditions in hand, we evaluated the substrate scope (Table 1). A variety of *N*-alkyl-*N*-arylacrylamides bearing *para* substituents of differing electronic character afforded the annulated products in consistently good yields (**4**−**11**), indicating that arene electronics exert minimal influence on radical cyclization. The reaction was also readily scalable to 2 mmol without a loss of efficiency (see Figure S2). In contrast, *ortho* substitution led to diminished yields (**12** and **13**), consistent with steric hindrance, and an acetal-protected arene remained compatible, delivering **14** in 31% yield. *meta* substitution resulted in the formation of a complex, non-separable mixture of isomeric products. Substitution at the alkene and nitrogen positions was likewise tolerated. Acrylamides bearing α-CF_3 (**15**) or α-benzyl (**16**) groups provided the corresponding oxindoles in 77 and 64% yields, respectively, and other *N*-alkyl groups furnished products **17** and **18** in moderate yields. Notably, β-phenyl acrylamide underwent annulation to give a six-membered product (**19**). Furthermore, tricyclic CF_3−BCP scaffolds were accessed under the same conditions in good yields (**20**−**22**). Finally, the extension to other radical acceptors demonstrated the generality of the transformation. An imide substrate afforded product **23** in 66% yield, while hydrazone derivatives underwent cyclization to furnish pyrazolones **24**−**26** in 37−43% yields, providing access to diverse heterocyclic architectures.

We next investigated the reaction mechanism. The addition of TEMPO completely suppressed the formation of **3**, and the TEMPO−BCP−CF_3 adduct was detected by HRMS, confirming radical involvement (see section 6.1 of the Supporting Information). To probe the origin of the radical, we examined the activation mode of thianthrenium salt **1**. The reduction potentials of the photocatalysts used (Figure 1A) are insufficient to reduce **1** (E_{red} = −1.89 V vs Fc^+/Fc), indicating that direct single-electron transfer (SET) from the excited photocatalyst is unlikely. Notably, the comparable efficiencies of 4CzIPN and 5CzBN, despite a 380 mV difference in the reduction potential, further support this conclusion. Next, Stern−Volmer analysis showed efficient quenching of 4CzIPN by **1** (K_{SV} = 64.3 M^{-1}), whereas no interaction was observed between 4CzIPN and acrylamide **2a** (Figure 1B). UV−Vis studies revealed that **1** absorbs at 312 nm, blue shifted relative to the 427 nm irradiation source (Figure 1C), excluding direct photoexcitation. Moreover, neither spectral overlap nor triplet energy considerations support the energy transfer. The triplet energy of **1** (E_T = 75.1 kcal mol^{-1})[12a] significantly exceeds those of the photocatalysts. Instead, UV−Vis spectra of mixtures of **1** and 4CzIPN (Figure 1D) showed a bathochromic shift consistent with the ground-state association. These data support the formation of an electron donor−acceptor (EDA) complex[14] between **1** and 4CzIPN, which mediates radical generation. To our knowledge, such EDA activation of a thianthrenium reagent by an organophotocatalyst has not previously been reported.[14a] Finally, a quantum yield Φ of 4.7 was determined, which is greater than 1 and consistent with a reaction pathway proceeding via a radical chain mechanism (*vide infra*).[15]

To further evaluate the mechanism for this transformation, we turned to dispersion-corrected DFT studies. Initially, we considered potential ground-state complexation (i.e., to form EDA complexes) between the 4CzIPN species (^{1}**PC**) and **1**. In total, we found the formation of five unique EDA complexes energetically favorable by ∼30 kcal/mol (Figure S11), supporting a charge transfer complex as the plausible activation pathway. Subsequent studies revealed that, after photoexcitation of 4CzIPN (^{1}**PC**), Dexter energy transfer[16] to **1** is not feasible due to a substantial energy gap of approximately 22 kcal/mol (Figure S12), consistent with the experimental findings. The electron density difference map (EDDM) obtained after the vertical excitation of the ground-state EDA complex revealed an electron depletion in the blue region (corresponding to the CF_3−BCP fragment) and an accumulation in the red region (corresponding to the 4CzIPN fragment), indicating a charge-transfer process within the complex (Figure 2 and Figure S13), which is in agreement with the experimental UV−vis experiment. This charge redistribution facilitates the generation of the BCP−CF_3 radical (**rad**$^\bullet$) and a 4CzIPN−thianthrenium intermediate, with Mulliken spin density localized on sulfur, supporting assignment of the radical cation to the thianthrenium fragment. Next, **rad**$^\bullet$ leads to regioselective and irreversible Giese-type radical addition to substrate **2a** via **TS1**, with a barrier of 7.9 kcal/mol to form **Int1**$^\bullet$ (downhill by 31.5 kcal/mol). In turn, **Int1**$^\bullet$ can undergo SET to form a carbocation or undergo radical cyclization. We found that radical cyclization (via **TS2**) proceeds via a modest barrier of 14.9 kcal/mol to generate cyclized **Int2**$^\bullet$. On the other hand, the alternative pathway leading to **Int1**$^+$ was found to be higher in energy (∼10 kcal/mol) than **TS2** and likely not operable. In turn, **Int2**$^\bullet$ can then undergo SET with **1** to form **rad**$^\bullet$, thianthrene (TT), and **Int3**$^+$, thereby enabling the radical chain and accounting for the experimentally observed Φ value. Finally, deprotonation of **Int3**$^+$ will lead to the desired product (downhill by 68.7 kcal/mol) and, at the same time, led to **rad**$^\bullet$ to re-enter the chain cycle. We found that a SET with another equivalent of the thianthrenium-based CF_3−BCP reagent (**1**) produced TT, and **rad**$^\bullet$ was only uphill by 2.7 kcal/mol with respect to **Int2**$^\bullet$.

In summary, we have developed a novel, transition-metal-free photochemical strategy for the synthesis of hybrid CF_3−BCP−oxindole scaffolds via radical cascade annulation. This method expands the chemical space of bioisosteric oxindoles by introducing the highly sought-after CF_3−BCP motif into a privileged heterocyclic framework using a sustainable and operationally simple protocol. The broad substrate scope, including the formation of complex tricyclic frameworks and compatibility with diverse radical acceptors, highlights the robustness and versatility of the transformation. Mechanistic studies revealed that the CF_3−BCP radical is generated through an unprecedented EDA complex between 4CzIPN and the thianthrenium salt, leading to a radical chain process. Experimental mechanistic studies have been found to be consistent with the DFT analysis. This approach represents a powerful platform for the late-stage introduction of two distinct and strategically valuable bioisosteres, bicyclo[1.1.1]-pentane and trifluoromethyl groups, into bioactive scaffolds.

■ ASSOCIATED CONTENT

Data Availability Statement

The data underlying this study are available in the published article and its Supporting Information.

Supporting Information

The Supporting Information is available free of charge at https://pubs.acs.org/doi/10.1021/acs.orglett.5c04624.

https://doi.org/10.1021/acs.orglett.5c04624
Org. Lett. 2026, 28, 248−253

Experimental section, including general experimental information, experimental procedures, characterization data, NMR, and DFT (PDF)

Accession Codes

Deposition Number 2496216 contains the supplementary crystallographic data for this paper. These data can be obtained free of charge via the joint Cambridge Crystallographic Data Centre (CCDC) and Fachinformationszentrum Karlsruhe Access Structures service.

AUTHOR INFORMATION

Corresponding Authors

Carolina Gimbert-Suriñach − *Department of Chemistry and Centro de Innovación en Química Avanzada (ORFEO−CINQA), Universitat Autònoma de Barcelona, Cerdanyola del Vallès, 08193 Barcelona, Spain;* orcid.org/0000-0002-4412-7607; Email: carolina.gimbert@uab.es

Adelina Vallribera − *Department of Chemistry and Centro de Innovación en Química Avanzada (ORFEO−CINQA), Universitat Autònoma de Barcelona, Cerdanyola del Vallès, 08193 Barcelona, Spain;* orcid.org/0000-0002-6452-4589; Email: adelina.vallribera@uab.es

Osvaldo Gutierrez − *Department of Chemistry and Biochemistry, University of California, Los Angeles, Los Angeles, California 90095, United States;* orcid.org/0000-0001-8151-7519; Email: o.gutierrez@ucla.edu

Albert Granados − *Department of Chemistry and Centro de Innovación en Química Avanzada (ORFEO−CINQA), Universitat Autònoma de Barcelona, Cerdanyola del Vallès, 08193 Barcelona, Spain;* orcid.org/0000-0002-5362-5966; Email: albert.granados@uab.es

Authors

Marta Gil-Ordóñez − *Department of Chemistry and Centro de Innovación en Química Avanzada (ORFEO−CINQA), Universitat Autònoma de Barcelona, Cerdanyola del Vallès, 08193 Barcelona, Spain*

Albert Gallego-Gamo − *Department of Chemistry and Centro de Innovación en Química Avanzada (ORFEO−CINQA), Universitat Autònoma de Barcelona, Cerdanyola del Vallès, 08193 Barcelona, Spain;* orcid.org/0000-0003-1278-9339

Yingmin Ji − *Department of Chemistry and Centro de Innovación en Química Avanzada (ORFEO−CINQA), Universitat Autònoma de Barcelona, Cerdanyola del Vallès, 08193 Barcelona, Spain*

Tapas Maity − *Department of Chemistry and Biochemistry, University of California, Los Angeles, Los Angeles, California 90095, United States*

Remy Lalisse − *Department of Chemistry and Biochemistry, University of California, Los Angeles, Los Angeles, California 90095, United States*

Elies Molins − *Institut de Ciència de Materials de Barcelona (ICMAB)−Consejo Superior de Investigaciones Científicas (CSIC), Campus UAB, 08193 Bellaterra, Spain;* orcid.org/0000-0003-1012-0551

Roser Pleixats − *Department of Chemistry and Centro de Innovación en Química Avanzada (ORFEO−CINQA), Universitat Autònoma de Barcelona, Cerdanyola del Vallès, 08193 Barcelona, Spain;* orcid.org/0000-0003-2544-732X

Complete contact information is available at: https://pubs.acs.org/10.1021/acs.orglett.5c04624

Author Contributions

†Albert Gallego-Gamo and Yingmin Ji contributed equally to this work. All authors have given approval to the final version of the manuscript.

Notes

The authors declare no competing financial interest.

ACKNOWLEDGMENTS

Support for this work under Grants PID2024-156087NB-I00, PID2021-124916NB-I00, PID2021-128496OB-I00, PID2021-124572OB-C32, and RED2022-134287-T funded by MCIN/AEI/10.13039/501100011033 (Spain) and 2021SGR00064 from AGAUR Generalitat de Catalunya is gratefully acknowledged. Osvaldo Gutierrez acknowledges NIH NIGMS (R35GM137797) for funding and the Hoffman2 Cluster at UCLA Office of Advanced Research Computing's Research Technology Group.

REFERENCES

(1) (a) Owen, B.; de Gaetano, M.; Gaffney, A.; Godson, C.; Guiry, P. J. Synthesis and Biological Evaluation of Bicyclo[1.1.1]pentane-Containing Aromatic Lipoxin A_4 Analogues. *Org. Lett.* **2022**, *24*, 6049−6053. (b) Auberson, Y. P.; Brocklehurst, C.; Furegati, M.; Fessard, T. C.; Koch, G.; Decker, A.; La Vecchia, L.; Briard, E. Improving Nonspecific Binding and Solubility: Bicycloalkyl Groups and Cubanes as *para*-Phenyl Bioisosteres. *ChemMedChem.* **2017**, *12*, 590−598.

(2) Kim, J. H.; Ruffoni, A.; Al-Faiyz, Y. S. S.; Sheikh, N. S.; Leonori, D. Divergent Strain-Release Amino-Functionalization of [1.1.1]-Propellane with Electrophilic Nitrogen-Radicals. *Angew. Chem., Int. Ed.* **2020**, *59*, 8225−8231.

(3) Subbaiah, M. A. M.; Meanwell, N. A. Bioisosteres of the Phenyl Ring: Recent Strategic Applications in Lead Optimization and Drug Design. *J. Med. Chem.* **2021**, *64*, 14046−14128.

(4) Pellicciari, R.; Raimondo, M.; Marinozzi, M.; Natalini, B.; Costantino, G.; Thomsen, C. (*S*)-(+)-2-(3′-Carboxybicyclo[1.1.1]-pentyl)-glycine, a Structurally New Group I Metabotropic Glutamate Receptor Antagonist. *J. Med. Chem.* **1996**, *39*, 2874−2876.

(5) (a) Stepan, A. F.; Subramanyam, C.; Efremov, I. V.; Dutra, J. K.; O'Sullivan, T. J.; DiRico, K. J.; McDonald, W. S.; Won, A.; Dorff, P. H.; Nolan, C. E.; Becker, S. L.; Pustilnik, L. R.; Riddell, D. R.; Kauffman, G. W.; Kormos, B. L.; Zhang, L.; Lu, Y.; Capetta, S. H.; Green, M. E.; Karki, K.; Sibley, E.; Atchison, K. P.; Hallgren, A. J.; Oborski, C. E.; Robshaw, A. E.; Sneed, B.; O'Donnell, C. J. Application of the bicyclo[1.1.1]pentane motif as a nonclassical phenyl ring bioisostere in the design of a potent and orally active γ-secretase inhibitor. *J. Med. Chem.* **2012**, *55*, 3414−3424. (b) Brown, D. G.; Boström, J. Analysis of Past and Present Synthetic Methodologies on Medicinal Chemistry: Where Have All the New Reactions Gone? *J. Med. Chem.* **2016**, *59*, 4443−4458.

(6) (a) Shire, B. R.; Anderson, E. A. Conquering the Synthesis and Functionalization of Bicyclo[1.1.1]pentanes. *JACS Au* **2023**, *3*, 1539−1553. (b) Kanazawa, J.; Uchiyama, M. Recent Advances in the Synthetic Chemistry of Bicyclo[1.1.1]pentane. *Synlett* **2019**, *30*, 1−11. (c) Sánchez-Sordo, I.; Barbeira-Arán, S.; Fañanás-Mastral, M. Enantioselective synthesis of chiral BCPs. *Org. Chem. Front.* **2024**, *11*, 916−928.

(7) Selected examples: (a) Cuadros, S.; Paut, J.; Anselmi, E.; Dagousset, G.; Magnier, E.; Dell'Amico, L. Light-Driven Synthesis and Functionalization of Bicycloalkanes, Cubanes and Related Bioisosteres. *Angew. Chem., Int. Ed.* **2024**, *63*, No. e202317333. (b) Nugent, J.; Arroniz, C.; Shire, B. R.; Sterling, A. J.; Pickford, H. D.; Wong, M. L. J.; Mansfield, S. J.; Caputo, D. F. J.; Owen, B.;

Mousseau, J. J.; Duarte, F.; Anderson, E. A. A General Route to Bicyclo[1.1.1]pentanes through Photoredox Catalysis. *ACS Catal.* **2019**, *9*, 9568−9574. (c) Lopchuk, J. M.; Fjelbye, K.; Kawamata, Y.; Malins, L. R.; Pan, C. M.; Gianatassio, R.; Wang, J.; Prieto, L.; Bradow, J.; Brandt, T. A.; Collins, M. R.; Elleraas, J.; Ewanicki, J.; Farrell, W.; Fadeyi, O. O.; Gallego, G. M.; Mousseau, J. J.; Oliver, R.; Sach, N. W.; Smith, J. K.; Spangler, J. E.; Zhu, H.; Zhu, J.; Baran, P. S. Strain-Release Heteroatom Functionalization: Development, Scope, and Stereospecificity. *J. Am. Chem. Soc.* **2017**, *139*, 3209−3226.

(8) (a) Purser, S.; Moore, P. R.; Swallow, S.; Gouverneur, V. Fluorine in medicinal chemistry. *Chem. Soc. Rev.* **2008**, *37*, 320−330. (b) Ni, C.; Hu, C. The unique fluorine effects in organic reactions: recent facts and insights into fluoroalkylations. *Chem. Soc. Rev.* **2016**, *45*, 5441−5454. (c) O'Hagan, D. Understanding organofluorine chemistry. An introduction to the C−F bond. *Chem. Soc. Rev.* **2008**, *37*, 308−319.

(9) Nair, A. S.; Singh, A. K.; Kumar, A.; Kumar, S.; Sukumaran, S.; Koyiparambath, V. P.; Pappachen, L. K.; Rangarajan, T. M.; Kim, H.; Mathew, B. FDA-Approved Trifluoromethyl Group-Containing Drugs: A Review of 20 Years. *Processes* **2022**, *10*, 2054.

(10) (a) Polites, V. C.; Badir, S. O.; Keess, S.; Jolit, A.; Molander, G. A. Nickel-Catalyzed Decarboxylative Cross-Coupling of Bicyclo[1.1.1]pentyl Radicals Enabled by Electron Donor−Acceptor Complex Photoactivation. *Org. Lett.* **2021**, *23*, 4828−4833. (b) Huang, W.; Keess, S.; Molander, G. A. A General and Practical Route to Functionalized Bicyclo[1.1.1]Pentane-Heteroaryls Enabled by Photocatalytic Multicomponent Heteroarylation of [1.1.1]-Propellane. *Angew. Chem., Int. Ed.* **2023**, *62*, No. e202302223. (c) Bunnell, A.; Milbauer, M. W.; Bento, J. V.; Taimoory, S. M.; Zimmerman, P. M.; Kalyani, D.; Piou, T.; Sanford, M. S. Mechanism-Guided Development of Directed C−H Functionalization of Bicyclo[1.1.1]pentanes. *J. Am. Chem. Soc.* **2025**, *147*, 20159−20167.

(11) (a) Boddy, A. J.; Bull, J. A. Stereoselective synthesis and applications of spirocyclic oxindoles. *Org. Chem. Front.* **2021**, *8*, 1026−1084. (b) Ding, K.; Lu, Y.; Nikolovska-Coleska, Z.; Wang, G.; Qiu, S.; Shangary, S.; Gao, W.; Qin, D.; Stuckey, J.; Krajewski, K.; Roller, P. P.; Wang, S. Structure-Based Design of Spiro-oxindoles as Potent, Specific Small-Molecule Inhibitors of the MDM2-p53 Interaction. *J. Med. Chem.* **2006**, *49*, 3432−3435.

(12) From redox-active esters: (a) Jin, Y.; Jiang, M.; Wang, H.; Fu, H. Installing amino acids and peptides on *N*-heterocycles under visible-light assistance. *Sci. Rep.* **2016**, *6*, 20068. (b) Tang, Q.; Liu, X.; Liu, S.; Xie, H.; Liu, W.; Zeng, J.; Cheng, P. *N*-(Acyloxy)phthalimides as tertiary alkyl radical precursors in the visible light photocatalyzed tandem radical cyclization of *N*-arylacrylamides to 3,3-dialkyl substituted oxindoles. *RSC Adv.* **2015**, *5*, 89009−89014. From halides: (c) Liu, F.; Li, P. Visible-Light-Promoted (Phenylsulfonyl)-methylation of Electron-Rich Heteroarenes and *N*-Arylacrylamides. *J. Org. Chem.* **2016**, *81*, 6972−6979. (d) Gao, X.; Dong, W.; Hu, B.; Gao, H.; Yuan, Y.; Xie, X.; Zhang, Z. Visible-light induced tandem radical cyanomethylation and cyclization of *N*-aryl acrylamides: access to cyanomethylated oxindoles. *RSC Adv.* **2017**, *7*, 49299−49302. (e) Majhi, J.; Granados, A.; Matsuo, B.; Ciccone, V.; Dhungana, R. K.; Sharique, M.; Molander, G. A. Practical, scalable, and transition metal-free visible light-induced heteroarylation route to substituted oxindoles. *Chem. Sci.* **2023**, *14*, 897−902. (f) Matsuo, B.; Majhi, J.; Granados, A.; Sharique, M.; Martin, R. T.; Gutierrez, O.; Molander, G. A. Transition metal-free photochemical C−F activation for the preparation of difluorinated-oxindole derivatives. *Chem. Sci.* **2023**, *14*, 2379−2385. From (Diacetoxyiodo)benzene: (g) Fu, W.; Xu, F.; Fu, Y.; Zhu, M.; Yu, J.; Xu, C.; Zou, D. Synthesis of 3,3-Disubstituted Oxindoles by Visible-Light-Mediated Radical Reactions of Aryl Diazonium Salts with *N*-Arylacrylamides. *J. Org. Chem.* **2013**, *78*, 12202−12206. From DMSO and MeCN: (h) Xie, Z.; Li, P.; Hu, Y.; Xu, N.; Wang, L. Visible-light-induced and iron-catalyzed methylation of *N*-arylacrylamides with dimethyl sulfoxide: a convenient access to 3-ethyl-3-methyl oxindoles. *Org. Biomol. Chem.* **2017**, *15*, 4205−4211. (i) Lu, M.; Zhang, T.; Tan, D.; Chen, C.; Zhang, Y.; Huang, M.; Cai, S. Visible-Light-Promoted Oxidative Alkylarylation of N-Aryl/Benzoyl Acrylamides Through Direct C−H Bond Functionalization. *Adv. Synth. Catal.* **2019**, *361*, 4237−4242. From boronic acids: (j) Li, X.; Han, M.-Y.; Wang, B.; Wang, L.; Wang, M. Visible-light-induced deboronative alkylarylation of acrylamides with organoboronic acids. *Org. Biomol. Chem.* **2019**, *17*, 6612−6619. From CH_2O systems: (k) Xia, D.; Li, Y.; Miao, T.; Li, P.; Wang, L. Visible-light-induced dual C−C bond formation via selective C(sp^3)−H bond cleavage: efficient access to alkylated oxindoles from activated alkenes and simple ethers under metal-free conditions. *Green Chem.* **2017**, *19*, 1732−1739. (l) Wei, W.-T.; Zhou, M.-B.; Fan, J.-H.; Liu, W.; Song, R.-J.; Liu, Y.; Hu, M.; Xie, P.; Li, J. H. Synthesis of Oxindoles by Iron-Catalyzed Oxidative 1,2-Alkylarylation of Activated Alkenes with an Aryl C(sp^2)−H Bond and a C(sp^3)−H Bond Adjacent to a Heteroatom. *Angew. Chem., Int. Ed.* **2013**, *52*, 3638−3641.

(13) (a) Alvarez, E. M.; Bai, Z.; Pandit, S.; Frank, N.; Torkowski, L.; Ritter, T. O-, N- and C-bicyclopentylation using thianthrenium reagents. *Nature Synth.* **2023**, *2*, 548−556. (b) Bai, Z.; Lansbergen, B.; Ritter, T. Bicyclopentylation of Alcohols with Thianthrenium Reagents. *J. Am. Chem. Soc.* **2023**, *145*, 25954−25961. (c) Zhang, G.; Luo, Z.; Mei, G.; Wang, H.; Ding, C. EDA Complex from BCP-Thianthrenium Salt: A Catalyst-Free Strategy To Access 1-Trifluoromethyl-3-quinoxaline Derivatives Bicyclo[1.1.1]pentanes. *Eur. J. Org. Chem.* **2024**, *27*, No. e202400386. (d) Pandit, S.; Ritter, T. Copper-Photoredox-Catalyzed C(sp^3)−C(sp^3) Reductive Cross-Coupling of Alkyl Bromides with BCP-Thianthrenium Reagents. *Angew. Chem., Int. Ed.* **2025**, *64*, No. e202506785.

(14) (a) Crisenza, G. E. M.; Mazzarella, D.; Melchiorre, P. Synthetic Methods Driven by the Photoactivity of Electron Donor−Acceptor Complexes. *J. Am. Chem. Soc.* **2020**, *142*, 5461−5476. (b) Sarró, P.; Gallego-Gamo, A.; Pleixats, R.; Vallribera, A.; Gimbert-Suriñach, C.; Granados, A. Access to Benzyl Oxindoles via Electron Donor−Acceptor Complex Photoactivation Using Thianthrenium Salts and Potassium Carbonate. *Adv. Synth. Catal.* **2024**, *366*, 2587−2595. (c) Zhao, H.; Cuomo, V. D.; Rossi-Ashton, J. A.; Procter, D. J. Aryl sulfonium salt electron donor−acceptor complexes for halogen atom transfer: Isocyanides as tunable coupling partners. *Chem.* **2024**, *10*, 1240−1251. (d) Patel, R. I.; Saxena, B.; Sharma, A. Photoactivation of Thianthrenium Salts: An Electron-Donor−Acceptor (EDA)-Complex Approach. *J. Org. Chem.* **2025**, *90*, 6617−6643. (e) van Dalsen, L.; Brown, R. E.; Rossi-Ashton, J. A.; Procter, D. J. Sulfonium Salts as Acceptors in Electron Donor−Acceptor Complexes. *Angew. Chem., Int. Ed.* **2023**, *62*, No. e202303104.

(15) Cismesia, M. A.; Yoon, T. P. Characterizing chain processes in visible light photoredox catalysis. *Chem. Sci.* **2015**, *6*, 5426−5434.

(16) Strieth-Kalthoff, F.; James, M. J.; Teders, M.; Pitzer, L.; Glorius, F. Energy transfer catalysis mediated by visible light: principles, applications, directions. *Chem. Soc. Rev.* **2018**, *47*, 7190−7202.

(17) (a) Wu, Y.; Kim, D.; Teets, T. S. Photophysical Properties and Redox Potentials of Photosensitizers for Organic Photoredox Transformations. *Synlett* **2022**, *33*, 1154−1179. (b) Sun, K.; Ge, C.; Chen, X.; Yu, B.; Qu, L.; Yu, B. Energy-transfer-enabled photocatalytic transformations of aryl thianthrenium salts. *Nat. Commun.* **2024**, *15*, 9693. (c) Shang, T.-Y.; Lu, L.-H.; Cao, Z.; Liu, Y.; He, W.-M.; Yu, B. Recent advances of 1,2,3,5-tetrakis(carbazol-9-yl)-4,6-dicyanobenzene (4CzIPN) in photocatalytic transformations. *Chem. Commun.* **2019**, *55*, 5408−5419.

(18) Dutta, S.; Erchinger, J. E.; Strieth-Kalthoff, F.; Kleinmans, R.; Glorius, F. Energy transfer photocatalysis: exciting modes of reactivity. *Chem. Soc. Rev.* **2024**, *53*, 1068−1089.

https://doi.org/10.1021/acs.orglett.5c04624
Org. Lett. 2026, 28, 248−253